Indian Journal of Chemistry
Vol. 63, November 2024, pp. 1112-1120
DOI: 10.56042/ijc.v63i11.12828

$FeVO_4$ nanoparticles: Powering synergistic hetero-Fenton photodegradation of methyl violet and enabling green chemical synthesis

S Thillainatarajan[a], L Firthawsha Yasmin[a], A Shalini[b], K Deepa[c], Krishnakumar Balu[d,e], I Muthuvel[a,f], Sabah Ansar[g], T Rajachandrasekar[a], G Thirunarayanan[f] & S Sivaselvan*[h]

[a] Photocatalysis Laboratory, Department of Chemistry, M. R. Government Arts College, Mannargudi 614 001, Tamil Nadu, India

[b] Department of Chemistry, SRM Institute of Science and Technology, Ramapuram, Chennai 600 089, India

[c] Department of Chemistry, Chellammal Women's College, Chennai 600 032, Tamil Nadu, India

[d] Saveetha School of Engineering, Saveetha Institute of Medical and Technical Sciences (SIMATS), Chennai 602 105, Tamil Nadu, India

[e] Departamento de Ingeniería y Ciencia de los Materiales y del Transporte, E. T .S. de Ingenieros, Universidad de Sevilla, Avda. Camino de los Descubrimientos s/n., 41092 Sevilla, Spain

[f] Advanced Photocatalysis Laboratory, Department of Chemistry, Annamalai University, Annamalainagar 608 002, Tamil Nadu, India

[g] Department of Clinical Laboratory Sciences, College of Applied Medical Sciences, King Saud University, P.O. Box 10219, Riyadh, 11433, Saudi Arabia

[h] Department of Physics, M. R. Government Arts College, Mannargudi 614 001, Tamil Nadu, India

E-mail: profsivaselvanphy@gmail.com, sivaselvan@mrgace.ac.in

Received 29 July 2024; accepted (revised) 22 October 2024

Various environmental problems have led to a shift in the way consumers go about their lives. Methyl violet (MV) being disposed of as a waste into water resources even in small quantities, creates certain hazards and environmental problems. $FeVO_4$ nanoparticles have been successfully synthesized by the reaction of Ferric nitrate and ammonium vanadate at 75°C for 1 h. It is then calcined at 500°C for 4 h. Characterization of $FeVO_4$ nanoparticles has been investigated by FTIR, XRD, SEM-EDS and colour mapping, and UV-DRS. The surface morphological study from SEM depicts rod-shaped particles with the formation of clusters. The photocatalytic activity of $FeVO_4$ has been studied by a heterogeneous Fenton-like process which is able to decompose the methyl violet effectively under UV-A light in the presence of a desired quantity of H_2O_2. The catalyst has been reused for multiple runs hence it can be used for economic industrial pilot studies and also the remarkable solid acidic nature of nano iron vanadate's catalytic activity is suitable for the synthesis of enones and sulphonamides.

Keywords: Methyl violet, Iron vanadate, Hetero-Fenton-like, Wastewater treatment, solid acid

Clean water is one of the most essential natural resources for humans, animals, and plants. With the rapid development of industries such as chemical, petrochemical, pharmaceutical, mining, semiconductor, and microelectronics around the world, the need for pure water as well as the purification of contaminated water has increased. Each of these industries requires a large quantity of water for processing, and subsequently, water discharged from them is contaminated with toxic organic pollutants. In addition, the increasing population of the world is also escalating the need for pure water for domestic purposes. The high population density and the level of industrialization have caused the hydrosphere to be polluted with organic and organic matter at an increasing rate. Decades of disposing of obnoxious waste without treatment on the land have created a serious groundwater contamination problem due to the leaching of metals from these wastes into water. Remediation of such contaminated water is an expensive process, and it is highly unlikely that developing countries will have enough resources to ensure sufficient clean water reserves. Semiconductor photocatalysts have created a revolution in wastewater treatment technologies, proving to be instrumental in the removal of obnoxious compounds and in splitting water for hydrogen production[1].

Fenton-assisted AOPs are accelerated by H_2O_2 and *in situ* generation of $^{\bullet}OH$ radicals in the aqueous phase. $^{\bullet}OH$ radicals are highly potent to oxidize the organic molecule quickly, economically, completely,

and effectively[2]. Similar to that of copper ferrite[3] ($CuFe_2O_4$) and iron poly vanadate[4] ($Fe_2V_4O_{13}$), $FeVO_4$ acts as the synergetic mechanistic pathway of hetero Fenton mineralization in the rapid generation of $^{\bullet}OH$. According to a literature survey, numerous solid acidic and nanocatalysts such as silica-sulphuric acid[5], Bi_2O_3-fly ash[6], fly-ash-sulphuric acid[7], flyash-PTS[8], fly-ash-phosphoric acid[9], Cu-zeolites[10,11], Fe-Bentonite[12], were employed for the synthesis of organic compounds like Enones[5], Imines[5], Pyrazolines[6,7], Sulphonamides[10,11], Quinoxaline[13], and Pyrimidines[14,15] derivatives. From this report and the acidic nature of iron vanadate, the authors investigated the catalytic activity of nano $FeVO_4$ for the synthesis of enone and sulphonamides. In this work, we report hetero-Fenton-like $FeVO_4$ nanoparticles for effective removal of methyl violet (MV) under UV-A light irradiation and also used as solid acid catalysis for green chemical synthesis.

Results and Discussion

Materials characterization

The phase structure of the as-prepared $FeVO_4$ sample obtained by powder XRD studies is shown in Fig. 1(I). The pattern of the as-prepared pure $FeVO_4$ sample is in good agreement with the standard values

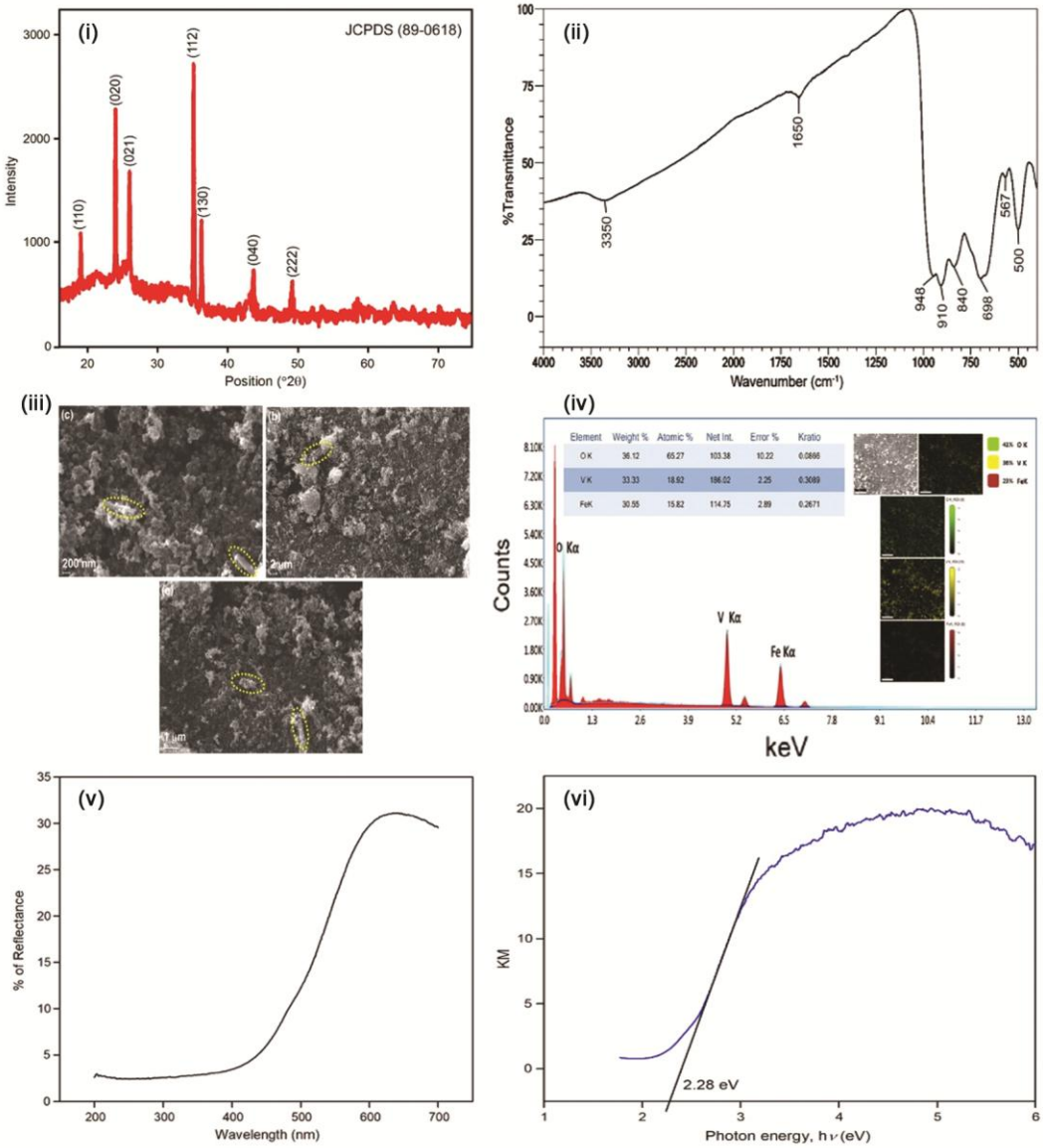

Fig. 1 — Characterization of $FeVO_4$ Nanomaterials (I) XRD patterns synthesized $FeVO_4$, (II) FT-IR spectrum of $FeVO_4$, (III) SEM images of $FeVO_4$: (a) 1 mm, (b) 2 mm and (c) 200 nm, (IV) EDX image of $FeVO_4$ and inset of colour mapping images of $FeVO_4$, (V) UV-DRS of $FeVO_4$, (VI) KM plot of $FeVO_4$.

of orthorhombic $FeVO_4$ (JCPDS No. 89-0618). The diffraction peaks were observed at 16.4,25.3,27.1,35. 0,36.9,43.2, and 49.2° were ascribed to the (110), (020), (021), (112), (130), (040) and (222) lattice planes of $FeVO_4$, respectively[8]. The Scherrer equation (Eqn.1) was employed for the calculation of the average crystallite size of $FeVO_4$ and it was found to be 66 nm.

$$D = k\lambda/\beta \cos\theta \quad \ldots (1)$$

Where D is the crystallite size, λ is the wavelength of the X-ray used; K is the shape factor, β is the full width at half maximum of the peak, and θ is the Bragg angle. Fig. 1(II) shows the FT-IR spectrum of $FeVO_4$, V–O terminal stretching observed at 948 cm^{-1}, 910 cm^{-1}, and 840 cm^{-1} while bridging V–O…Fe stretching can be observed at 698 cm^{-1}. Additionally, V–O–V deformation was observed at 500 cm^{-1} [16,17]. This proves $FeVO_4$ to be an ionic compound consisting of VO_4^{3-} anions and Fe^{3+} cationic species[18,19]. The surface OH stretching and bending vibrations of $FeVO_4$ were observed at 3350 and 1650 cm^{-1}, respectively. Fig. 1(III) shows the morphological features of the synthesized $FeVO_4$ particles and that they are round and rod-like structures[20]. The presence of the elements Fe, V, and O in the catalyst is confirmed by EDX analysis from the selected area. The EDX analysis revealed that the respective atoms are present in the prepared sample Fig. 1(IV). To confirm the presence of these elements, $FeVO_4$ was analyzed by elemental mapping shown in the inset of Fig. 1(IV). The various colored areas indicate the Fe-, V-, and O-enriched areas of the sample. The diffused reflectance spectrum of prepared $FeVO_4$ is shown in Fig. 1(V). DRS spectroscopy is used to reveal the electronic state of a photocatalyst material and is very useful for photocatalysis.

The as-prepared $FeVO_4$ shows strong visible-light absorption and a corresponding optical band gap of 2.28eV [Fig. 1(VI)] [21].

Photocatalytic activity

The photocatalytic activity of the $FeVO_4$ catalyst was evaluated by the degradation of MV under UV-A light. Controlled experiments under different reaction *p*H were carried out and the results are displayed in Fig. 2a. The *p*H of the dye wastewater discharged varies; it is therefore important to study the role of *p*H on the degradation efficiency. Experiments were carried out at a range of *p*H, from 4 to 9 with a constant amount of the dye (4×10^{-4}M) and catalyst (1 g L^{-1}). Fig. 2a illustrates the increase in the degradation from 67 to 97% for the increase of *p*H from 4 to 7(60 min). Further, increase in *p*H above 7 decreases the degradation efficiency.

The effect of catalyst $FeVO_4$ loading on the photodegradation of dye is a crucial parameter in optimizing the degradation efficiency. Increasing the loading of $FeVO_4$ generally enhances the availability of active sites, thereby improving the generation of reactive oxygen species (ROS) such as hydroxyl radicals (•OH) under light irradiation. This, in turn, accelerates the breakdown of dye molecules. The effect of catalyst loading was studied by varying the catalyst amount from 0.6 g L^{-1} to 1.8 g L^{-1} (Fig. 2b). The amount of catalyst increased from 0.6 g L^{-1} to 1.0 g L^{-1}, and the degradation efficiency increased. Further, increasing the catalyst amount declined the degradation efficiency. The optimum catalyst loading for efficient removal of MV dye is found to be 1.0 g L^{-1}.

The maximum degradation of MV is observed at *p*H 7. Hence, *p*H 7 is optimal for this heterogeneous photo-Fenton degradation of MV, which overcomes the drawback of the narrow *p*H range of homogeneous Fenton catalysis. The degradation of MV with $FeVO_4$ at *p*H 7 at different H_2O_2 concentrations was studied. The addition of H_2O_2 (5–20 mmol) increased the *pseudo*-first-order rate constant from 0.0185 to 0.0804 min^{-1} in the mineralization of MV (Fig. 2c). Further increase of H_2O_2 concentration above 20 mmol decreased the rate of mineralization of MV (20min). Hence, 20 mmol of H_2O_2 is the optimum concentration in the mineralization of MV[22].

Many researchers have investigated the effect of initial dye concentration on the mineralization in solution. An increase of the initial dye concentration from 1 to 5×10^{-4} M decreases the degradation rate constant from 0.1237 to 0.0423 min^{-1} in 10 min (Fig. 2d). The rate of degradation relates to the •OH (hydroxyl radical) formation on the catalyst surface and the probability of •OH reacting with the dye molecule. For all initial dye concentrations, the catalyst amount and light intensity are the same. Since the generation of hydroxyl radical remains constant, the probability of the dye molecule reacting with hydroxyl

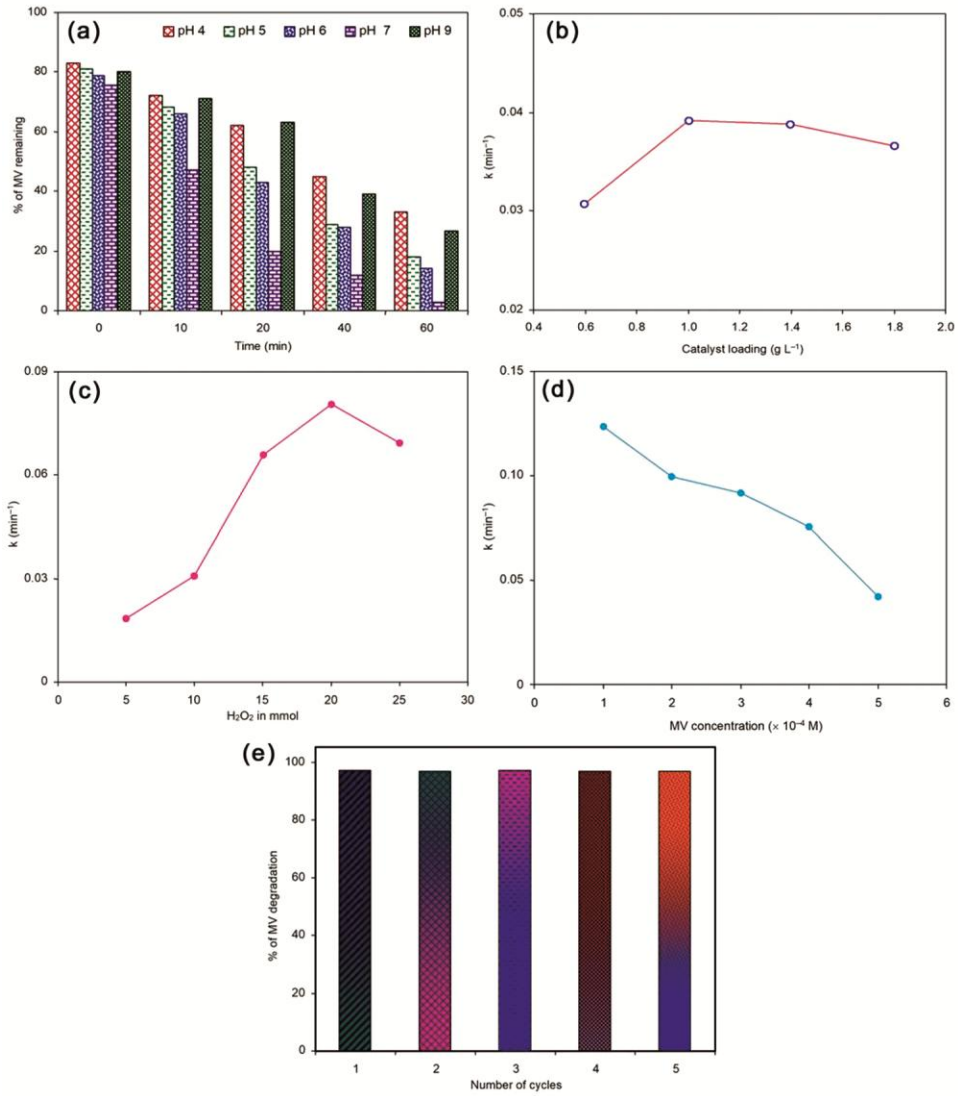

Fig. 2 — Photocatalytic activity of $FeVO_4$, (a) Effect of initial solution *p*H,(b) Effect of catalyst loading (c) Effect of H_2O_2, (d) Effect of initial dye concentration,(e) Long-term stability

radical decreases. At high initial dye concentrations, the path length of photons entering into the solution also decreases[4]. However, it should be pointed out that even at a high initial concentration of MV (5×10^{-4} M), about 90% of dye removal was achieved in 20 min. This indicates that the $FeVO_4$ catalyst can also work well at high initial concentrations of MV.

The reusability of the heterogeneous photo-Fenton catalyst was tested and the results are shown in Fig. 2e. About 97% of dye removal takes place at 60 min in the first cycle. The same catalyst was separated, dried, and used again. In the second cycle, 97% of the dye was removed at 60 min. The third cycle also gave 97% dye removal at 60 min. The fourth cycle gave 97% dye removal and the fifth cycle gave 97% dye removal. Thus, there was no significant decrease in degradation even in the fifth cycle. Hence, the catalyst is reusable.

Table 1 — The $FeVO_4$ assisted COD measurements under optimum conditions

Time (min)	0	30	60	90	120
COD reduction (%)	0	36.21	59.71	86.9	98.1

The reaction mechanism between iron-containing materials and H2O2 is described by the following reactions[23].

To confirm the mineralization of the dye, COD measurements were made for the degradation of MV in the presence of $FeVO_4$ under optimum conditions. The reductions in values for the dye at different times of UV irradiation are given in Table 1. COD values

show that 98.1% reduction of the MV dye at 120 min UV irradiation. These results confirm the mineralization of the dye with the $FeVO_4$ process.

$$Fe^{3+} + H_2O_2 \rightarrow Fe^{2+} + {}^{\bullet}OOH + H^{+} \quad \ldots (2)$$

$$Fe^{2+} + H_2O_2 \rightarrow Fe^{3+} + {}^{\bullet}OH + OH^{-} \quad \ldots (3)$$

Furthermore, there are anions that combine with iron cations to form heterogeneous Fenton-like catalysts. Moreover, hydroxyl radicals are produced by catalytic reactions that involve V and H2O2. These reactions are summarized below:

$$V^{5+} + H_2O_2 \rightarrow V^{4+} + {}^{\bullet}OOH + H^{+} \quad \ldots (4)$$

$$V^{4+} + H_2O_2 \rightarrow V^{5+} + {}^{\bullet}OH + OH^{-} \quad \ldots (5)$$

The recycling of Fe^{3+} from Fe^{2+} by reaction (3) and V^{5+} from V^{4+} by reaction (5) is several orders of magnitudes lower than reaction (2) and reaction (4), respectively. Reaction (3) and reaction (5) are considered as the rate-limiting steps of the iron cycling and vanadium cycling, respectively. The presence of UV light increases the rates of reactions (3) and (5), and simultaneously accelerates the regeneration of Fe^{3+} and V^{5+}. As a result, the Fe^{3+}/Fe^{2+} and V^{5+}/V^{4+} cycles are well maintained in the $FeVO_4$-H_2O_2 system and ${}^{\bullet}OH$ is produced faster, which means that the role of incident light increases significantly the H_2O_2 efficiency in producing ${}^{\bullet}OH$ according to reaction (2)–(5). Consequently, the oxidative capacity of the $FeVO_4$–H_2O_2 system greatly improves, and the degradation rate of MV increases owing to the irradiation with UV light (Scheme 1).

Synthetic utility of $FeVO_4$ catalyst

As mentioned in the experimental section, the authors investigated the effect of nano-$FeVO_4$ catalyst on the synthesis of enones. In this condensation, the obtained yields of the enones are more than 75%. This condensation undergoes acidic catalyzed aldol condensation type. The possible reaction mechanism was illustrated in Scheme 2. This condensation follows the acid-catalyzed crossed Aldol condensation. The first step is the enolization of ketone by the protonation of carbonyl oxygen from the acidic site of the iron vanadate catalyst. The second step is the attack of aldehyde carbonyl carbon by the enol form of the ketone and an oxonium ion was formed. The third step is the protonation of oxonium ions. The fourth step is the removal of water by beta elimination afforded the enones.

The physical constants, yield, and time of reactions are presented in Table 2. The synthesized enones purities were examined with their physical constants and spectroscopic data reported in the literature earlier. All data were well accepted in the synthesized enones.

Also, the authors examined the catalytic action of nano-$FeVO_4$ catalyst by synthesis of sulphonamides.

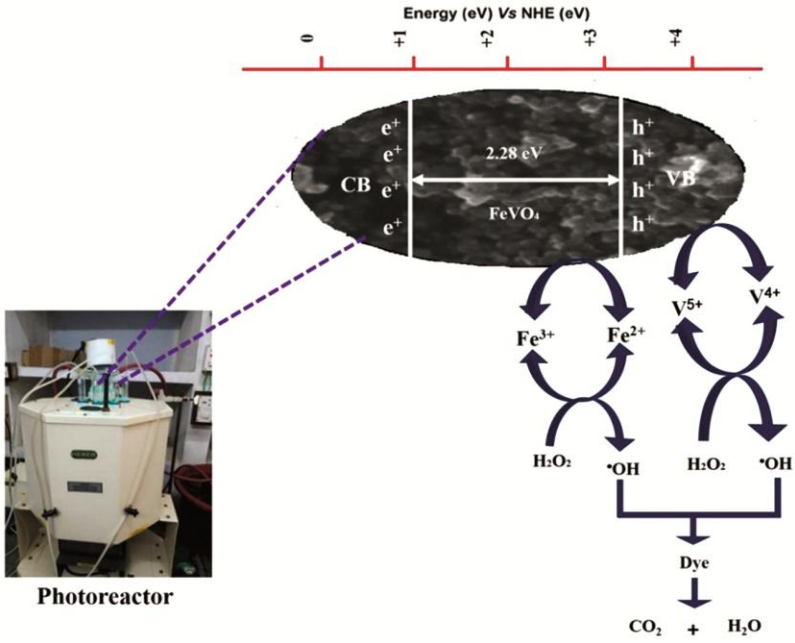

Scheme 1 — Photocatalytic degradation mechanism

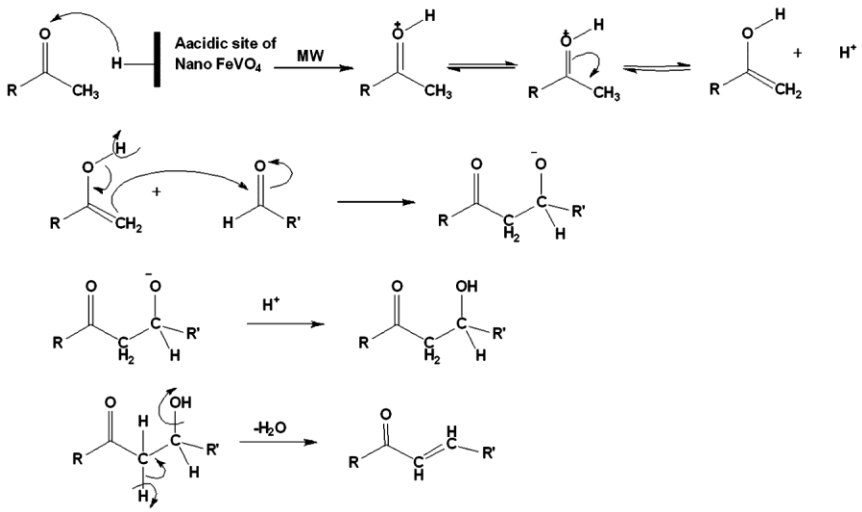

Scheme 2 — The plausible mechanism for the formation of enones

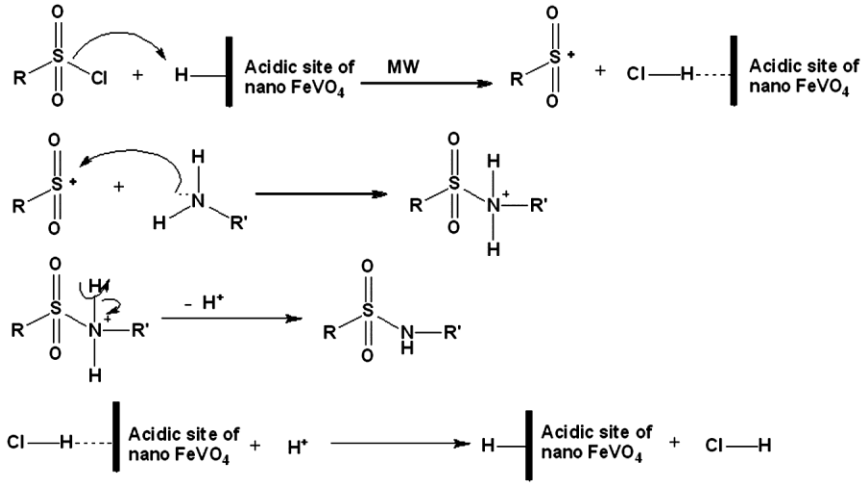

Scheme 3 — The plausible mechanism for the formation of sulphonamides mediated by $FeVO_4$

Table 2 — The melting point, yield, and time of reactions of enones mediated by the $FeVO_4$ catalyst

S. No.	R	R′	Yield (%)	Time (min)	m.p. (°C)
1	Phenyl	Phenyl	88	4	56-57(55-56) (Ref. 9)
2	9*H*-Fluorenyl	Phenyl	85	5	149-151(149-150) (Ref. 23)
3	2-Naphthyl	Phenyl	88	3.5	105-106(104-105) (Ref. 8)
4	Piperidinophenyl	Phenyl	79	5.5	190-191(191-192) (Ref. 9)
5	2-Pyrenyl	Phenyl	80	4	162–163 (161–162) (Ref. 24)
6	4-Ethoxyphenyl	Phenyl	81	5	72-73(72-73) (Ref. 25)
7	2-Hydroxy-1-naphthyl	Phenyl	77	5.5	102-103(101-102) (Ref. 26)
8	4-Biphenyl	Phenyl	82	4	156-157(155-156) (Ref. 27)
9	1-Pyrene	Phenyl	80	3	177–178 (176–177) (Ref. 28)
10	3,4-Dimethoxyphenyl	Phenyl	83	3.5	73-74(74–75) (Ref. 29)

As stated in the experimental section, the yield of the sulphonamides is more than 60%. This reaction goes with a well-known simple condensation route. The possible reaction mechanism is shown in Scheme 3. The first step consists of the formation of aryl sulfoxide cation by abstraction of chloride ion on the acidic site of the catalyst. The second step is the nucleophilic attack of aryl sulfoxide by amine to form the positive charge on the amine nitrogen atom. Then it loses a proton to afford the sulfonamide. The proton

combined with chloride ion to form hydrogen chloride and the catalyst was regenerated.

The physical constants, yield, and time of reactions of sulfonamides are presented in Table 3. The synthesized sulfonamides purities were examined with their physical constants and spectroscopic data reported in the literature earlier. All data were well accepted for the synthesized sulfonamides.

Experimental Section

The commercial dye Methyl Violet (MV) (C.I – 42535), AnalaR H_2O_2 (30 w/w%) (SD fine), ferric nitrate (Qualigens), ammonium metavanadate (Qualigens), HCl, H_2SO_4, and NaOH (Fisher Scientific) were used as received. Ferrous ammonium sulfate, AnalaR silver sulfate (Himedia), mercury (II) sulfate (Merck 90%), potassium dichromate, and ferroin indicator (SD fine) solutions were used as received for chemical oxygen demand analysis. The experimental solution was prepared using double-distilled deionized water.

Preparation of $FeVO_4$

Typically, 0.35 g NH_4VO_3 was dissolved into 50 mL of deionized water to form a transparent solution (A). Following this, 1.21 g of $Fe(NO_3)_3.9H_2O$ was dissolved in 50 mL of deionized water to form a transparent solution (B). Then B was poured into A with magnetic stirring, which generated lots of yellow precipitate. Then, NH_3 solution was added with constant stirring until *p*H 8 was reached and maintained at 75°C for 1h. After cooling to RT, the precipitate was collected and washed with deionized water and ethanol and dried at 100°C in a vacuum oven for 12 h. The precipitate was calcined in a muffle furnace at 500°C for 4 h. The resulting powder was ground and stored at RT for further use (Scheme 4).

Synthesis of Enones

Equimolar quantities of aryl ketones with 10 mg of nano $FeVO_4$ catalyst were subjected to microwave irradiation for 3-5 minutes in the period of 30 seconds (Scheme 5) in the microwave oven (Ragatech, RG 31L Scientific Microwave oven, 230 V A/C, 50 Hz, 2450 Hz, 1200 rpm (beam reflector)). The feasibility of the reaction was monitored by the Thin Layer Chromatogram. After completion of the reaction, the reaction mixture was extracted with 10 mL of dichloromethane. The catalyst was separated by simple filtration. Evaporation of the extract gave the

Table 3 — The physical constants, yield, and time of reactions of sulfonamides

S.No.	R	R'	Yield (%)	Time (min)	m.p. (°C)
1	Phenyl	2-Hydroxy-4-amino benzoic acid	68	4	275-276(276) (Ref. 11)
2	4-Chlorophenyl	Phenyl	65	4.5	308-310(310) (Ref. 11)
3	4-Methoxyphenyl	Phenyl	62	5	301-302(301) (Ref. 11)
4	2-Nitrophenyl	Phenyl	69	5	313-314(314) (Ref. 11)
5	Phenyl	2,4-Difluoroaniline	70	5	(163-165) (Ref. 26)
6	4-Chlorophenyl	Phenyl	74	4.5	(189-191) (Ref. 26)
7	4-Methoxyphenyl	Phenyl	73	4	(182-185) (Ref. 27)
8	4-Nitrophenyl	Phenyl	75	4	9180-182) (Ref. 27)
9	4-Methylphenyl	Phenyl	78	4	198-199(200-204) (Ref. 28)
10	4-Methylphenyl	4-Bromophenyl	68	5	117-118(116-118) (Ref. 28)

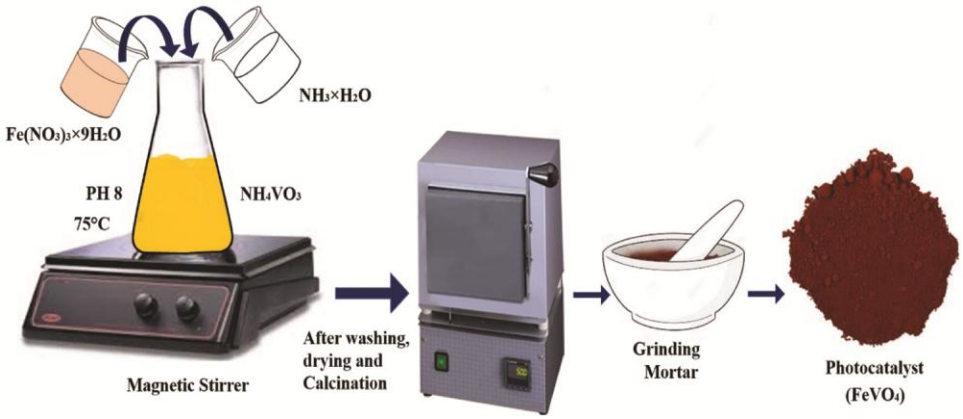

Scheme 4 — Preparation of $FeVO_4$ Nanomaterials

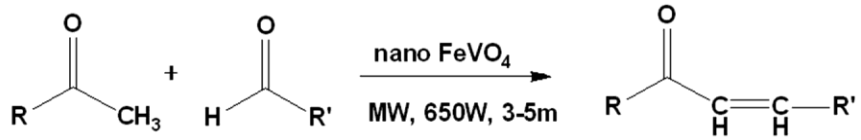

Scheme 5 — Synthesis of some enones using nano $FeVO_4$ catalyst assisted crossed aldol condensation

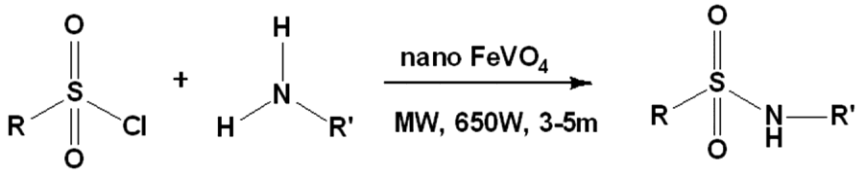

Scheme 6 — Synthesis of sulphonamides using nano $FeVO_4$ catalyst-assisted condensation of aryl sulphonyl chloride and amines

crude enones. The crude was recrystallized with ethanol afforded the glittering enones and these are stored in a desiccator. Spectral data of the selected compounds were given in Supporting information.

Synthesis of Sulphonamides

An equimolar concentration of sulfonyl chlorides with 10 mg of nano $FeVO_4$ catalyst was subjected to microwave irradiation for 3-5 minutes in the period of 30 seconds (Scheme 6) in the microwave oven (Ragatech, RG 31L Scientific Microwave oven, 230 V A/C, 50 Hz, 2450 Hz, 1200 rpm (beam reflector)). During the reaction 0.1 mL of triethylamine was added to neutralize the formation of hydrochloride. The feasibility of the reaction was monitored by the Thin Layer Chromatogram. After completion of the reaction, the reaction mixture was extracted with 10 mL of *n*-hexane. The catalyst was separated by simple filtration. Evaporation of the extract gave the crude sulphonamides. The crude was washed 2 times with *n*-hexane and kept in a desiccator. Spectral data of the selected compounds were given in Supplementary Information.

Photo-degradation experiments and characterization techniques

Heber multi-lamp photoreactor model HML-MP 88 is used for photodegradation. The details of the photoreactor and photocatalytic experiment with 50 mL of dye solution and the appropriate quantity of photocatalyst under UV-A light (365 nm) irradiation were reported earlier.[4] Instrumentation details of FT-IR, XRD, SEM-EDX, and UV-DRS have already been given earlier[29,30]. COD was determined using the literature procedure[31].

Conclusion

A heterogeneous Fenton $FeVO_4$ catalyst was prepared by the co-precipitation method. It was used as a photocatalyst for the degradation of Methyl Violet (MV) under UV light. $FeVO_4$ catalyst shows efficient photocatalytic activity for the mineralization of MV dye. The XRD pattern of the as-prepared pure $FeVO_4$ sample is in good agreement with the standard values of orthorhombic $FeVO_4$. FT-IR spectrum of the as-prepared $FeVO_4$ sample, the characteristic absorption bands are observed. The morphological features of the synthesized $FeVO_4$ were characterized by SEM showing that the particles are spherical and rod-shaped. The as-prepared $FeVO_4$ shows strong visible-light absorption with an optical band gap of 2.28 eV. It is expected that the strong visible-light absorption contributes to the efficiency of the direct solar light-assisted photo-Fenton process. In the presence of $FeVO_4$, optimum *p*H and catalyst concentration for MV mineralization with UV light were found to be *p*H 7 and 1 g L^{-1}, respectively. The reusability for $FeVO_4$ was analyzed, and almost 97% of degradation was observed for all five cycles. Hence, the $FeVO_4$ catalyst was found to be reusable and it could be used for the treatment of dye wastewater. The complete mineralization was confirmed by COD (98%) reduction.

Acknowledgments

The authors thank the Researchers Supporting Project number (RSP2024R169), King Saud University, Riyadh, Saudi Arabia for financial support.

Supplementary Information

Supplementary information is available in the website http://nopr.niscpr.res.in/handle/123456789/58776.

References

1 Liao C H, Huang C W & Wu J C, *Catalyst*, 2 (2012) 490.
2 Zhang M H, Dong H, Zhao L, Wang D X & Meng D, *Sci Total Environ*, 670 (2019) 110.

3 Hamdan N, Haija M A, Banat F & Eskhan A, *Desal Water Treat*, 69 (2017) 268.
4 Gowthami K, Suppuraj P, Thirunarayanan G, Krishnakumar B, Sobral A J F D N, Swaminathan M & Muthuvel I, *Iranian Chem Comm*, 6 (2018) 97.
5 Thirunarayanan G & Vanangamudi G, *Arkivoc*, 12 (2006) 58.
6 Thirumurthy K & Thirunarayanan G, *Arabian J Chem*, 11(2018) 443.
7 Thirunarayanan G, Mayavel P &Thirumurthy K, *Spectrochim Acta*, 91A (2012) 18.
8 Arulkumarana R, Kamalakkannana D, Sundararajana R, Vijayakumara S, Thirumurthy K, Mayavelb P & Thirunarayanan G, *Annales Univ Mariae Curie Sklodowska*, 67 (2012) 45.
9 Joseph S J, Ranganathan K, Suresh R, Arulkumaran R, Sundararajan R, Kamalakkannan D & Viveksarathi K, *Mat Sci Appl Chem*, 34 (2017) 12.
10 Ranganathan K, Kamalakkannan D, Suresh R, Sakthinathan S P, Arulkumaran R, Sundararajan R & Thirunarayanan G, *Mat Today: Proceed*, 22 (2020) 1196.
11 Dineshkumar S, Thirunarayanan G, Mayavel P & Muthuvel I, *Ovidius Univ Annals Chem*, 27 (2016) 22.
12 Muthuvel I, Dineshkumar S, Thirumurthy K, Rajasri S & Thirunarayanan G, *Indian J Chem*, 55B (2016) 252.
13 Thirunarayanan G, Muthuvel I & Sathiyendiran V, *Int Lett Chem Phys Astro*, 19 (2014) 198.
14 Divya J, Gayathri P, Muthuvel I &Thirunarayanan G, *Indian J Chem*, 62 (2023) 1178.
15 Divya J, Gayathri P, Muthuvel I & Thirunarayanan G, *Ovidius Univ Annal Chem*, 34 (2023) 150.
16 Kumar A, Kumar A, Sharma G, Naushad M, Stadler F J, Ghfar A A, Dhiman P & Saini R V, *J Clean Prod*, 165 (2017) 431.
17 Heydari A, Sheykhan M, Sadeghi M & Radfar I, *Inorg Nano-Metal Chem*, 47 (2017) 248.
18 Nithya V D, Selvan R K, Sanjeeviraja C, Radheep D M & Arumugam S, *Mat Res Bull*, 46 (2011) 1654.
19 Vuk A S, Orel B, Drazic G, Decker F & Colomban P, *J Sol-gel Sci Tech*, 23 (2002) 165.
20 Tong Y & Ang P S, *Adv Mater Res*, 486 (2012) 124.
21 Thirunarayanan G, Vanangamudi G, *E-J Chem*, 4 (2007) 90.
22 Muthuvel I, Thirunarayanan G, Thangaraj V, Sundaramurthy N, Rajalakshmi S & Usha V, *Mater Today: Proceed*, 43 (2021) 2203.
23 Nalini S, Sekar K G, Srinivasan S, Muthuvel I & Thirunarayanan G, *J Sci Res*, 15 (2023) 783.
24 Vanangamudi G, Subramanian M, Jayanthi P, Arulkumaran R, Kamalakkannan D &Thirunarayanan G, *Arabian J Chem*, 9 (2016) S717.
25 Sekar K G, Janaki P, Muthuvel I, Usha V, Thirumurthy K & Thirunarayanan G, *Mat Today: Proc*, 43 (2021) 2208.
26 Mala V, Muthuvel I, Thirunarayanan G & Usha V, *Mat Today: Proc*, 43 (2021) 2117.
27 Sekar K G & Thirunarayanan G, *Int Lett Chem Phys Astro*, 8 (2013) 249.
28 Dineshkumar S, Muthuvel I, Mayavel P, Markanadan R, Usha V, &Thirunarayanan G, *Indian J Chem*, 60B (2021) 1373.
29 Suppuraj P, Parthiban S, Swaminathan M & Muthuvel I. *Mat Today: Proc*, 15 (2019):429.
30 Muthuvel I, Gowthami K, Thirunarayanan G, Suppuraj P, Krishnakumar B, do Nascimento Sobral A J & Swaminathan M, *Int J Ind Chem*, 10 (2019) 77
31 Muthuvel I, Krishnakumar B & Swaminathan M, *Indian J Chem*, 53A (2014) 672.